The Rayleigh–Bénard Convection in Rarefied Gases

Carlo Cercignani*, Maria Cristina Giurin† and Jens Struckmeier‡

Abstract

In the present paper we investigate the Rayleigh–Bénard convection in rarefied gases and demonstrate by numerical experiments the transition from purely thermal conduction to a natural convective flow for a large range of Knudsen numbers from 0.02 downto 0.001. We address to the problem how the critical value for the Rayleigh number defined for incompressible viscous flows may be translated to rarefied gas flows. Moreover, the simulations obtained for a Knudsen number $Kn = 0.001$ and Froude number $Fr = 1$ show a further transition from regular Rayleigh–Bénard cells to a pure unsteady behaviour with moving vortices.

1 Introduction

The Rayleigh–Bénard convection is a well–known example in continuum fluid dynamics for a temperature–driven flow phenomena, which yields a natural convective flow: assume that a viscous fluid layer is enclosed between two horizontal walls, where the lower one is heated from below. If the temperature gradient between the two walls exceeds a certain critical value, there occurs a transition from purely thermal conduction to a natural convective flow together with the formation of the so–called Rayleigh–Bénard cells. Due to the vortices appearing in each Rayleigh–Bénard cell, a convective flow is generated up- and downwards along the normal direction of the horizontal walls.

An independent measure for the transition from thermal conduction to convective flow is given by the Rayleigh number Ra, which should exceed the critical value $Ra_c \geq 1708$ in the case of incompressible viscous fluids. This value was already derived by Rayleigh itself in 1916 [22] applying a stability analysis for the incompressible Navier–Stokes equations in the Boussinesq approximation (see also [3]).

The transition to natural convection for incompressible viscous fluids is widely studied in the literature: see [1], [28] for experimental data, [13], [20] for numerical simulations on the basis of the incompressible Navier–Stokes equations. Recently, several authors investigate the existence of a Rayleigh–Bénard instability in rarefied gases, see Refs. [11], [23] and [24], and demonstrate by numerical experiments the formation of a vortical structure. Moreover, in Refs. [23] and [24], the authors discussed the characterization of this first transition in terms of the critical value Ra_c for the Rayleigh number.

In the present paper we give a further investigation on the Rayleigh–Bénard problem and the transition to natural convection in rarefied gases. In particular, we give a wide range of numerical experiments applying a particle simulation scheme for the monoatomic Boltzmann equation and discuss the definition of the Rayleigh number in rarefied gas flows.

*Dipartimento di Matematica, Politecnico di Milano, Italy
†Dipartimento di Matematica U. Dini, Università di Firenze, Italy
‡Department of Mathematics, University of Kaiserslautern, Germany

Remark 1
An investigation of the Rayleigh–Bénard problem by means of molecular dynamics and the microscopic simulation of instabilities was given by Mareschal in Ref. [16] as well as by Mareschal and Kestermont in Ref. [17].

As mentioned above, we will study in the following the Rayleigh–Bénard convection in rarefied gases: we consider a monoatomic rarefied gas enclosed between two parallel plates with two different temperatures T_{up} and T_{down} (see Fig. 1).

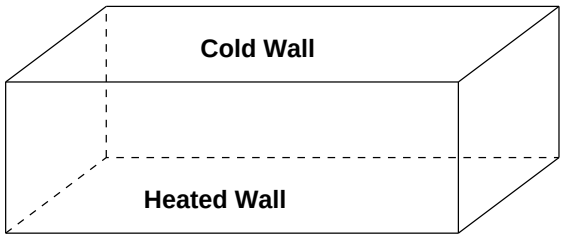

Fig. 1 Rayleigh–Bénard Problem

Moreover, we assume that the gas is heated from below, i.e. $T_{up} = T_C < T_H = T_{down}$, and there acts a (gravitational) force $F = m(0,0,g)^t$, which accelerates each gas particle vertically downwards.
Then, the Rayleigh–Bénard problem in rarefied gases is described by the time–dependent Boltzmann equation with external force on $\Omega \subset I\!R^3$ given by

$$f_t + \mathbf{v}\nabla_{\mathbf{x}} f - g\partial_{v_z} f = Q(f) \tag{1.1}$$

where $\mathbf{x} = (x,y,z) \in \Omega$ and $\mathbf{v} = (v_x, v_y, v_z) \in I\!R^3$ are the spatial coordinates and velocities, respectively, and $\Omega = [0, L_x] \times [0, L_y] \times [0, L_z]$. The collision operator in (1.1) – assuming that f describes the number density of the rarefied gas – is given by [6]

$$Q(f) = \frac{1}{m} \int\int k(|\mathbf{v} - \mathbf{v}_*|, \mathbf{n}) \{f' f'_* - f f_*\} \mathrm{d}\mathbf{n} \mathrm{d}\mathbf{v}_* \quad f' = f(t, \mathbf{x}, \mathbf{v}'),\ f'_* = f(t, \mathbf{x}, \mathbf{v}'_*) \ etc.$$

where $k = |\mathbf{v} - \mathbf{v}_*| \sigma(|\mathbf{v} - \mathbf{v}_*|, \mathbf{n})$ and σ denotes the differential cross section describing the interactions between particles.
Equation (1.1) is equiped with an initial condition at time $t = 0$ in the form

$$f(0, \mathbf{x}, \mathbf{v}) = f_0(\mathbf{x}, \mathbf{v})$$

and some boundary conditions on $\partial\Omega$: at the two parallel plates we assume diffusive reflection with complete thermal accomodation according to the temperatures T_H and T_C, i.e.

$$\begin{aligned} f(t, \mathbf{x}, \mathbf{v}) &= f(t, x, y, 0, \mathbf{v}) = M_H(\mathbf{v}) \int\limits_{v'_z < 0} |v'_z| f^-(t, x, y, 0, \mathbf{v}') \mathrm{d}\mathbf{v}' \quad \text{if } v_z > 0 \\ f(t, \mathbf{x}, \mathbf{v}) &= f(t, x, y, L_z, \mathbf{v}) = M_C(\mathbf{v}) \int\limits_{v'_z > 0} |v'_z| f^+(t, x, y, 0, \mathbf{v}') \mathrm{d}\mathbf{v}' \quad \text{if } v_z < 0 \end{aligned}$$

where M_C and M_H denote (scaled) halfspace Maxwellians

$$M_X(\mathbf{v}) = \frac{1}{2\pi T_X} \exp\left(-\frac{\mathbf{v}^2}{2T_X}\right), \quad X \in \{C, H\}$$

For the other walls involved in our problem we use specular reflecting boundary conditions in x–direction and periodicity in the y–direction.

Remark 2
Like stated in the previous work by Stefanov and Cercignani [24] this corresponds to periodic boundary conditions on a larger domain $\bar{\Omega}$ with size $[0, 2L_x] \times [0, L_y] \times [0, L_z]$ and therefore reduces the computational effort performing numerical simulations on $\bar{\Omega}$.

The paper is organized as follows: in Section 2, we discuss the definition of the Rayleigh number Ra, when studying the Rayleigh–Bénard convection in a rarefied gas, because there exists various possibilities to define the parameters appearing in the definition of the Rayleigh number itself. In particular, the different possibilities yield – in contrast to incompressible viscous fluids – even large deviations in the Rayleigh number and this makes it more complicated to define a reliable critical value Ra_c, where a first transition occurs.
Section 3 gives a brief overview on the numerical scheme, which is used in the present paper to simulate the monoatomic Boltzmann equation and we mainly focuse on the way how to include the external gravitational force in the (stochastic) particle approach. Finally, we present a large number of numerical simulations in Section 4: in Section 4.1, we give results obtained from numerical simulations for Knudsen numbers between 0.05 and 0.008 and various values for the temperature ratio T_C/T_H and the Froude number. Here, we discuss how the critical value $Ra_c = 1708$ from continuum flows can be used to characterize the transition to natural convective flow in rarefied gases. In Section 4.2, we give first results on numerical simulations performed at a Knudsen number $Kn = 0.001$ and show how a second transition to an unsteady motion with moving vortices appears in the Rayleigh–Bénard problem, which was not observed before by the authors in Refs. [23] and [24].

2 The Rayleigh Number in Rarefied Gases

As mentioned in the introduction, an independent measure for the transition from pure thermal conduction to natural convection in the Rayleigh–Bénard problem is the Rayleigh number, which should exceed the critical value $Ra_c = 1708$ in the case of an incompressible viscous fluid. In this section we address to the problem how one may translate the Rayleigh number to the case of a rarefied gas.
The classical definition of the Rayleigh number Ra in continuum theory, like found in Ref. [7], is given by

$$Ra = \frac{g\alpha\beta}{K\nu} d^4 \tag{2.1}$$

where g denotes the acceleration due to gravity, d the depth of the layer, i.e. in our problem the distance between the two horizontal walls. Moreover, $\beta(= |dT/dz|)$ denotes the uniform adverse temperature gradient, which is assumed to be fixed, α, K, and ν are the coefficients for the volume expansion, the thermometric conductivity and the kinematic viscosity, respectively.
In order to "translate" the definition of the Rayleigh number given by (2.1) from continuum theory to rarefied gases, it is important to understand how to choose the coefficients in the definition of the Rayleigh number and there arise directly the following two problems: the first is connected with the coefficient α for the volume expansion, the second one with the definition of the coefficient of thermometric conductivity K.
In Ref. [7], the author used the so–called Boussinesq approximation, that is to assume that the physical properties of the fluid, which are involved in the Rayleigh number are temperature independent, except the density (hypothesis of incompressible fluid), in which the coefficient of thermometric conductivity is related with the heat conduction coefficient k via the formula $K = k/(\rho_0 c_v)$, where ρ_0 is the density and c_v the specific heat at constant volume. On the other

hand in Ref. [9], the authors define the thermometric conductivity coefficient for incompressible fluids by $K = k/(\rho_0 c_p)$, where c_p is the specific heat at constant pressure.
We observe, that the difference between these two definitions is negligible for incompressible fluids, but it is not in the case of a compressible one. In Ref. [4], the authors consider the case of a dilatable fluid together with the definition $K = k/(\rho_0 c_p)$. They find, that the critical value Ra_c can be different from 1708, which defines the critical value for the first transition for incompressible fluid. In the case of compressible fluids, the difference in the definition of the coefficient of thermometric conductivity yields a difference in the definition of Ra of a factor c_v/c_p, and for a monoatomic gas one has $c_p/c_v = 5/3$. Hence, we will use in the following both definitions for Ra and denote them by Ra_{c_v} and Ra_{c_p}, respectively.
In a second step, we have to choose the coefficient α, which defines the volume expansion and even here there are several possibilities to do this: for a dilute gas, we know that $\alpha = \bar{T}^{-1}$ and one possible value for $\bar{T}$ is to take the mean value $(T_H + T_C)/2$ of the two wall temperatures T_C and T_H. Another possibility is to use $\bar{T}$ as the spatial average given by

$$\bar{T} = \frac{1}{d} \int_0^d T(x) \mathrm{d}x$$

where $T(x)$ is given as the solution of the Navier–Stokes equations

$$\frac{\partial}{\partial x} \left(k(T) \frac{\partial T}{\partial x} \right) = 0$$

where $k(T) = c\sqrt{T}$ assuming a hard–sphere interaction law. Hence, this choice yields the temperatur $\bar{T}$ as

$$\bar{T} = \frac{3}{5} \frac{T_H^{5/2} - T_C^{5/2}}{T_H^{3/2} - T_C^{3/2}} \tag{2.2}$$

and we denote these two volume expansion coefficients by α_1 and α_2, respectively.

Remark 3
In the classical Rayleigh–Bénard problem from continuum theory, the temperature ratio T_C/T_H is typically close to unity. Hence, the difference between the mean value $(T_C + T_H)/2$ and the spatial average $\bar{T}$ given by (2.2) is negligible. Moreover, if the heat conduction coefficient k is assumed to be weakly dependent of the temperature, both definitions for $\bar{T}$ are nearly equal, even for larger temperature ratios.

Together with the definition of the critical coefficients in the expression (2.1) of the Rayleigh number, i.e. the volume expansion coefficient α as well as the coefficient of thermometric conductivity, one may relate the Rayleigh number Ra to the characteristic parameters of the Rayleigh–Bénard problem in rarefied gases. These dimensionless parameters are the Knudsen number Kn of the rarefied gas, the Froude number Fr, which relates the thermal speed with the acceleration vertically downwards due to gravity, and the temperature ratio between the heated and cooled walls. In particular, we have the following expressions for the Knudsen number based on the mean free path $\lambda_0 = (\sqrt{2}\pi\sigma^2 n_0)^{-1}$ and the Froude number Fr, based on the thermal speed $v_H = \sqrt{2RT_H}$, where $R = k_B/m$, k_B the Boltzmann constant and m the mass,

$$Kn = \frac{\lambda}{d}, \qquad \mathrm{Fr} = \frac{v_H^2}{gd}.$$

Remark 4
In the following, we will also consider the scaled Froude number $Fr^* = Fr/Kn$.

Finally, we have to specify the expressions for the viscosity coefficient μ and the heat conduction coefficient k of a rarefied gas: using the well–known Chapman–Enskog approximation [8], we have a viscosity coefficient $\mu = 1.016\mu^{(1)}$, where

$$\mu^{(1)} = \frac{5}{16\sigma^2}\left(\frac{k_B m T}{\pi}\right)^{\frac{1}{2}} = \frac{5}{16}\lambda\rho_0 v_H\sqrt{\pi}.$$

and the kinematic viscosity ν is given by $\nu = \mu/\rho_0$. In Ref. [8], we even find a first approximation $k^{(1)}$ for the heat conduction coefficient in the form

$$k^{(1)} = \frac{5}{2}\mu^{(1)}c_v = \frac{3}{2}\mu^{(1)}c_p$$

In the case for which $K = k/(\rho_0 c_v)$, we obtain

$$K^{(1)} = \frac{5}{2}\nu^{(1)},$$

if we consider $K = k/(\rho_0 c_p)$, we have

$$K^{(1)} = \frac{3}{2}\nu^{(1)}.$$

Together with $\beta = \Delta T/d$, and $k = 1.02513k^{(1)}$, we finally obtain the formulas

$$Ra_{c_v} = 3.13\cdot\alpha\frac{\Delta T}{FrKn^2}\left(\frac{2}{5}\right)$$
$$Ra_{c_p} = 3.13\cdot\alpha\frac{\Delta T}{FrKn^2}\left(\frac{2}{3}\right)$$

and the ratio is given by $Ra_{c_v}/Ra_{c_p} = 3/5 = c_v/c_p$.
Finally, we like to clarify, that the authors of Refs. [23] and [24] used a slightly different definition for the Rayleigh number in rarefied gases: in Ref. [23], Sone et al. used a Rayleigh number in the form

$$Ra = \frac{16}{\pi}\frac{(1-r)}{rFrKn^2}, \quad r = T_C/T_H \tag{2.3}$$

whereas Stefanov and Cercignani [24] defined the Rayleigh number as

$$Ra = \frac{512}{75\pi}\frac{(1-r)}{rFrKn^2}, \quad r = T_C/T_H \tag{2.4}$$

In both definitions, it is assumed, that the volume expansion coefficient is given by $\alpha = 1/T_C$ and both used implicitely the definition of Curle and Davies [9] to define the thermometric conductivity coefficient in the form $K = k/(\rho_0 c_p)$. Hence, besides the difference in the volume expansion coefficient, the Rayleigh numbers given in (2.3) and (2.4) corresponds to the value Ra_{c_p} given above. The difference in the definitions (2.3) and (2.4) comes from the fact, that Sone et al. used a simplified BGK–model to study the Rayleigh–Bénard convection, whereas Stefanov and Cercignani considered, like in the present investigation, the full Boltzmann equation together with the hard–sphere interaction model [2].

3 Simulation Schemes for the Boltzmann Equation

Numerical simulation schemes for rarefied gas flows are nearly exclusively based on (stochastic) particle methods, like, e.g., the Direct Simulation Monte Carlo (DSMC) schemes by Bird [5] or the Finite–Pointset Method (FPM) as presented in Ref. [18]. In the following we shortly recall the main ideas of such schemes – following the ideas given in [18] – and explain how to include the gravitational force in the free flow of particles.
The kinetic density function $f(t, \mathbf{x}, \mathbf{v})$ on the phase space $\Omega \times I\!R^3$ is approximated using a stochastic particle system $(\mathbf{x}_i(t), \mathbf{v}_i(t))_{i=1,\ldots,n}$ of particles, where $\mathbf{x}_i$ and $\mathbf{v}_i$ denote the spatial coordinate and velocity of the i–th particle, respectively. Then, the time evolution of the particles is derived from a time and space–discretized form of the Boltzmann equation (1.1). In particular, one uses a so–called splitting method in order to separate the free–flow of particles, described by the left hand side of (1.1), from binary collisions defined by the collision operator $Q(f)$ in the Boltzmann equation.
The splitting method is defined as follows: take the discrete time steps $t_k = k\Delta t$, $k = 0, 1, \ldots$ and solve on the time intervals $[t_k, t_{k+1}]$ successively the two equations

$$\tilde{f}_t + \mathbf{v} \cdot \nabla_x \tilde{f} - g\partial_{v_z} \tilde{f} = 0, \ \tilde{f}(t_k, \mathbf{x}, \mathbf{v}) = f(t_k, \mathbf{x}, \mathbf{v}) \tag{3.1}$$

$$\tilde{f}(f_t) = Q(f), \ f(t_k, \mathbf{x}, \mathbf{v}) = \tilde{f}(t_{k+1}, \mathbf{x}, \mathbf{v}) \tag{3.2}$$

On the level of the (stochastic) particle system, the first part of the splitting method, Eq. (3.1) yields the particle trajectories

$$\ddot{\tilde{\mathbf{x}}}_i = (0, 0, -g)^t, \ i = 1, \ldots, n \tag{3.3}$$

which reduces by direct computation to the formula

$$\tilde{\mathbf{x}}_i(t_{k+1}) = \mathbf{x}_i(t_k) + \Delta t \mathbf{v}_i(t_k) + \frac{(\Delta t)^2}{2}(0, 0, -g)^t \quad \tilde{\mathbf{v}}_i(t_{k+1}) = \mathbf{v}_i(t_k) + \Delta t(0, 0, -g)^t$$

The boundary conditions are incorporated into Eq. (3.3) on the basis of a single gas–surface interaction between one particle and the wall.

Remark 5
In contrast to the Boltzmann equation without force term, the particle trajectories are no longer straight lines, but parabolic curves in the z–component. Hence, the treatment of the boundary conditions becomes more complicated, in particular, if $g \ll 1$.

The derivation of binary collisions for the particle system from Eq. (3.2) is quite more complicated and the crucial part in the numerical simulation. The main problem arises from the locality of the collision operator in the space variable. To overcome this problem, one has to introduce a smoothed collision operator Q^δ defined by

$$Q^\delta(f)(\mathbf{v}) = \int_\Omega \int_{I\!R^3} \int_{S^2_+} \beta(\mathbf{x}, \mathbf{x}_*) k(|\mathbf{v} - \mathbf{v}_*|, \mathbf{n}) \{f' f'_* - f f_*\} \mathrm{d}\mathbf{n} \mathrm{d}\mathbf{v}_* \mathrm{d}\mathbf{x}_*$$

$$f' = f(t, \mathbf{x}, \mathbf{v}'), \ f'_* = f(t, \mathbf{x}_*, \mathbf{v}'_*) \ etc.$$

using an appropriate smoothing kernel $\beta(\mathbf{x}, \mathbf{x}_*)$. The most simple choice for $\beta(\mathbf{x}, \mathbf{x}_*)$, which is also used in the present paper, is to use a spatial grid to perform collisions, i.e. we use the smoothing kernel $\beta(\mathbf{x}, \mathbf{x}_*)$ defined by

$$\beta(\mathbf{x}, \mathbf{x}_*) = \sum_{i=1}^{m} \frac{\mathcal{X}_{\Omega_i}(\mathbf{x}, \mathbf{x}_*)}{Vol(\Omega_i)} \tag{3.4}$$

where $\mathcal{T}_h = \{\Omega_1, \ldots, \Omega_m\}$ denotes a disjoint partition of the domain Ω, i.e. $\Omega = \bigcup_{i=1}^{m} \Omega_i$ and $\Omega_i \cap \Omega_j = \emptyset$, if $i \neq j$.

With the special choice of the smoothing kernel given in (3.4), the second part of the splitting method is reduced to a system of spatial–homogeneous Boltzmann equation on $\mathcal{T}_h$, because two particles can only undergo a binary collision, if they are located in the same cell. Moreover, during this part of the splitting method, the spatial coordinates of the particles will remain constant.

The collision process itself is derived from a time–discretized Boltzmann equation for each cell $\Omega_i \in \mathcal{T}_h$ and typically one uses an explicit Euler step to discretize the time derivative $\partial f/\partial t$, but one may even use an implicit Euler step as well as a mixed implicit–explicit Crank–Nicholson–type scheme. Passing to the weak form of the discretized equation, one finally obtains a collision mechanism on each cell $\Omega_i \in \mathcal{T}_h$ on the basis of the given particle approximation. Here, we refer the reader to Refs. [18] and [19].

The numerical simulations presented in the Section 4 are based on partially dimensionless quantities: the spatial domain is kept fixed for different Knudsen numbers, i.e. the space coordinates are not scaled with respect to the mean free path of the gas. On the other hand, we use scaled velocities and temperatures; scaled with respect to the thermal speed $v_H = \sqrt{2RT_H}$ and the hot–wall temperature T_H. This scaling yields a (scaled) gravitational acceleration of the form $\hat{g} = g/v_H^2 = 1/(Fr^* \lambda_\infty)$.

For typical values Kn and Fr* used in the following, the parameter $\hat{g}$ turns out to be much less than unity and this influences the way how to treat boundary conditions in the free–flow step of the splitting method given by Eq. (3.3): if the particle undergoes an interaction with the upper or lower wall, one has to determine the intersection point of the particle trajectory with the, e.g., $z = 0$–plane and to recompute the remaining time step after the interaction. This means to solve the quadratic equation

$$\frac{\hat{g}}{2}\Delta\tau^2 - v_i\Delta\tau + z_i = 0 \tag{3.5}$$

for the time variable $\Delta\tau$. If $\hat{g} \ll 1$, Eq. (3.5) may be considered as singular perturbed and the correct solution (which remains finite as $\hat{g} \to 0$) may be computed using an asymptotic expansion (see Ref. [25]).

4 Numerical Results and Discussion

In the following we give numerical results for the Rayleigh–Bénard convection in rarefied gases using the particle schemes described in the previous section. In particular, we performed two different sets of simulations

- two–dimensional computations for Knudsen numbers $Kn \geq 0.008$ in order to validate the previous results obtained by Stefanov and Cercignani [24] and to give a more complete set of data
- two–dimensional computations for a Knudsen number $Kn = 0.001$ in order to investigate the behaviour of the Rayleigh–Bénard convection close to the continuum limit covered by the Navier–Stokes equations.

The numerical results are obtained using a three–dimensional program with only one single cell in the y–direction and specular reflection at the two walls in y–directions as well as using a real two–dimensional program. The results obtained from the two different approaches are qualitatively the same[1].

Remark 6
All simulations are performed using massively–parallel systems with a fully parallelized particle code, where the parallelization is done similar to the approach given in Ref. [26]: the computational domain is divided into subdomains along the x–direction and neighbouring processors need to communicate during the free–flow step of the splitting method. In particular, the simulation were done on a parallel system nCUBE 2S with up to 64 processors installed at the Department of Mathematics, University of Kaiserslautern and a Cray T3E with up to 256 processors installed at the Regional University Computer Center, University of Stuttgart.

4.1 Two–Dimensional Simulations for Kn ≥ 0.008

Some results from numerical simulations, where one expects the first transition to natural convective flow with the formation of Rayleigh–Bénard cells and vortices are presented in the following. The simulations are performed on a fixed spatial domain with size 300 x 100 using three different spatial grids

- a coarse grid with 192 x 64 cells for Kn ≥ 0.02,
- a fine grid with 384 x 128 cells for $0.008 <$ Kn < 0.02,
- a super fine grid with 576 x 192 cells for Kn $= 0.008$

Hence, the size of a single cell is 1.5625 for the coarse, 0.78125 for the fine and 0.52083 for the super fine grid, where a Knudsen number $Kn = 0.01$ yields a mean free path $\lambda = 1.0$. Even when using massively–parallel systems like in the present investigation, the computational effort to perform numerical simulations is quite high, because one has to perform long–time simulations in order to detect the first transition. Moreover, one should vary, keeping the Knudsen number Kn fixed, the temperature gradient ΔT as well as the Froude number Fr in order to be able to characterize the first transition. Therefore, the simulations are performed with an averaged number of 10 particles per cell, which yields about $1.2 \cdot 10^5$ particles on the coarse, $4.8 \cdot 10^5$

[1] In a subsequent paper the authors will give numerical results for the Rayleigh–Bénard convection in rarefied gase using fully three–dimensional simulations

particles on the fine and $1.1 \cdot 10^6$ particles on the super fine grid. The (scaled) discrete time step for all simulation is equal to the spatial grid size.
We tabulate the different simulations in terms of the characteristic parameters cases in Tab. 1.

Table 1 Numerical results for $Kn \in [0.008, 0.05]$ and various parameters T_C/T_H and Fr^*.

Kn	T_C/T_H	Fr^*	stable	Ra_{c_v,α_1}	Ra_{c_v,α_2}	Ra_{c_p,α_1}	Ra_{c_p,α_2}
0.05	0.05	12	yes	1510	1307	2517	2179
0.05	0.1	12	yes	1365	1216	2276	2027
0.05	0.1	200	yes	81	72	136	121
0.03	0.1	50	yes[1]	1517	1351	2529	2252
0.03	0.1	100	yes	758	675	1264	1126
0.03	0.1	300	yes	252	225	421	375
0.03	0.1	400	yes[2]	189	168	316	281
0.02	0.1	50	yes[1]	5121	4560	8536	7601
0.02	0.1	100	no	2560	2280	4268	3800
0.02	0.1	300	no	853	760	1422	1266
0.02	0.1	400	yes[2]	640	570	1067	950
0.02	0.2	50	yes[1]	4173	3869	6955	6448
0.02	0.2	100	no	2086	1934	3477	3224
0.02	0.2	200	yes[2]	1043	967	1738	1612
0.02	0.4	100	yes	1341	1300	2235	2167
0.01	0.1	100	yes[1]	20487	18243	34145	30406
0.01	0.1	200	no	10243	9121	17072	15203
0.01	0.1	800	no	2560	2280	4268	3800
0.01	0.1	1600	yes	1280	1140	2134	1900
0.01	0.2	100	yes	16693	15477	27822	25795
0.01	0.2	200	no	8346	7738	13911	12897
0.01	0.2	400	no	4173	3869	6955	6448
0.01	0.2	800	yes	2086	1934	3477	3224
0.01	0.4	200	yes	5365	5202	8942	8671
0.008	0.1	120	yes[1]	33345	29693	55575	49489
0.008	0.1	200	no	20007	17816	33345	29693
0.008	0.1	1600	no	2500	2227	4168	3711
0.008	0.1	3200	yes[2]	1250	1113	2084	1855
0.008	0.2	120	yes	27170	25190	45283	41984
0.008	0.2	200	no	16302	15114	27170	25190
0.008	0.2	800	no	4075	3778	6792	6297
0.008	0.2	1300	yes	2508	2325	4180	3875
0.008	0.4	200	tr[3]	10479	10161	17466	16936

[1]The resulting purely conductive state has an decreasing density profile from the lower to the upper wall
[2]The resulting purely conductive state has an increasing density profile from the lower to the upper wall
[3]The resulting steady–state shows no clear transition to natural convective flow, see also Fig. 4

We give some interpretation of the results shown in Tab. 1. First of all, the simulations show a first transition – with respect to the Knudsen number – to natural convective flow at $Kn = 0.02$, for the larger values $Kn = 0.03$ and $Kn = 0.05$, the resulting steady–state is detected as purely conductive.

Remark 7
In Ref. [24], Stefanov and Cercignani reported a first transition at a Knudsen number $Kn = 0.01$. For the reduced BGK–model, Sone et al. [23] observed a transition to natural convective flow even for larger Knudsen numbers than $Kn = 0.02$.

If we consider at $Kn = 0.02$ a fixed Froude number $Fr^* = 100$, the resulting critical Rayleigh number seems to be in good agreement with the value predicted by continuum theory, if the Rayleigh number is based on the definition given in Ref. [7]. On the other hand, we observe that, assuming a fixed temperature ratio $T_C/T_H = 0.1$, the critical value for the Rayleigh number is less than $Ra_c = 1708$, for all possible definitions of the Rayleigh number discussed in Section 2. If the Knudsen number is decreased to $Kn = 0.01$ and $Kn = 0.008$, the results of Tab. 1 show that the "window" for a transition to natural convective flow is increased with respect to the temperature ratio as well as the Froude number. The critical value for a transition is in agreement with the value from continuum theory only for a fixed temperature ratio $T_C/T_H = 0.1$, for other combinations, e.g. a fixed Froude number, the critical value turns out to be larger than $Ra_c = 1708$. This result indicates, that the Rayleigh number seems to be not appropriate to detect the transition in the Rayleigh–Bénard problem in rarefied gases uniformly with respect to all characteristic parameters, i.e. the Knudsen number, the temperature ratio as well as the Froude number.
As an example for the transition to natural convective flow, we give some pictures on the vortical structures obtained from the simulations given in Tab. 1: Fig. 2 shows the vortical structures obtained at the end of the numerical simulation for $Kn = 0.02$, Froude number $Fr^* = 200$ and a temperature ratio $T_C/T_H = 0.1$.

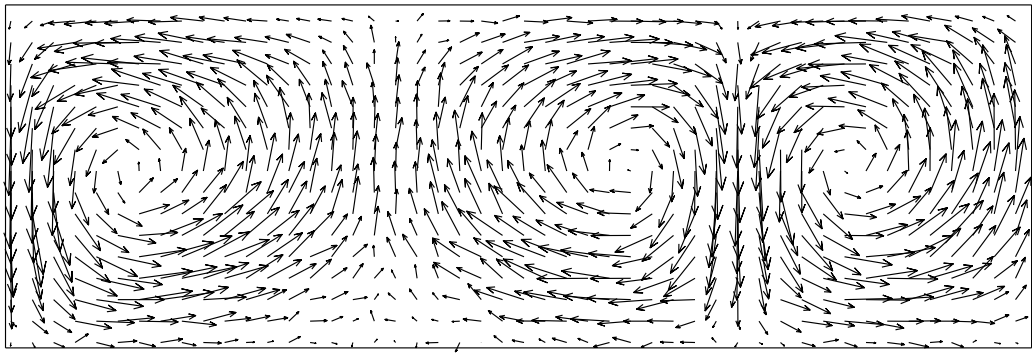

Fig. 2: Vortical structures for $Kn = 0.02$, $Fr^* = 200$ and $T_C/T_H = 0.1$

The corresponding iso–lines for the temperature and density field are presented in Fig. 3.

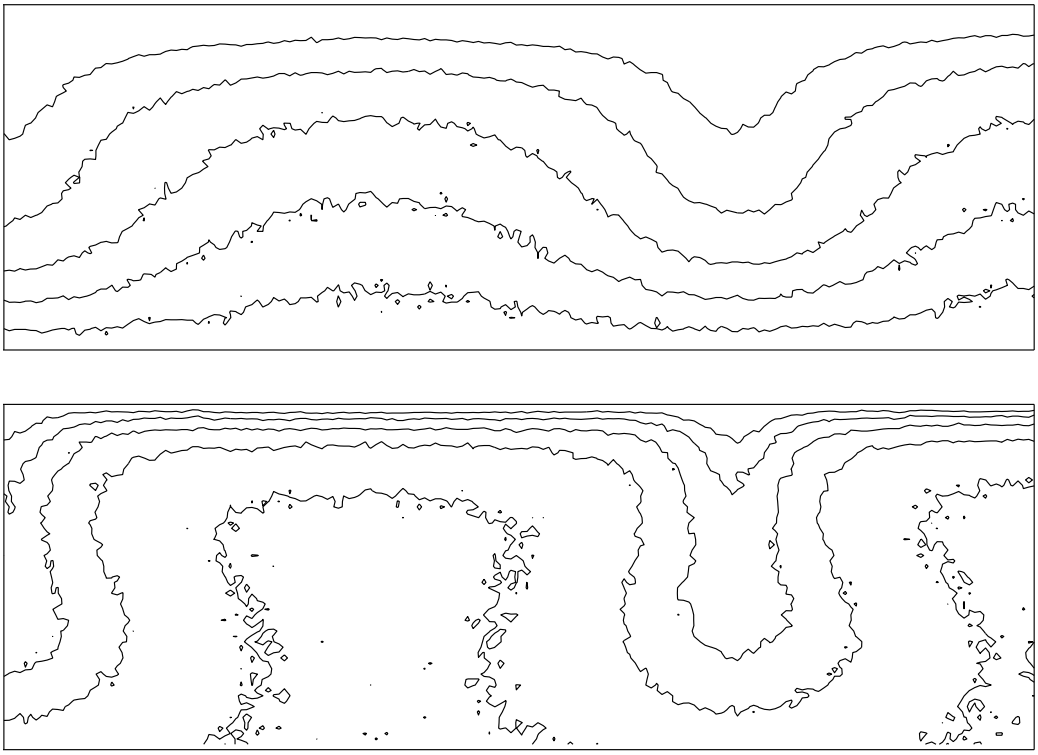

Fig. 3: Iso–Temperature (up) and Density Lines (down) for $Kn = 0.02$, $Fr^* = 200$ and $T_C/T_H = 0.1$

In Fig. 4 we give the vortical structures obtained, after a fixed number of discrete time steps, for the particular case $Kn = 0.008$, $Fr^* = 200$ and different temperature ratios between the upper and lower wall. Here, the macroscopic moments are computed as a mean time average over 500 subsequent steps, starting after 13.500 time steps.
For a fixed temperature ratio $T_C/T_H = .35$, Fig. 5 shows the vortical structures at different times during the numerical simulation.

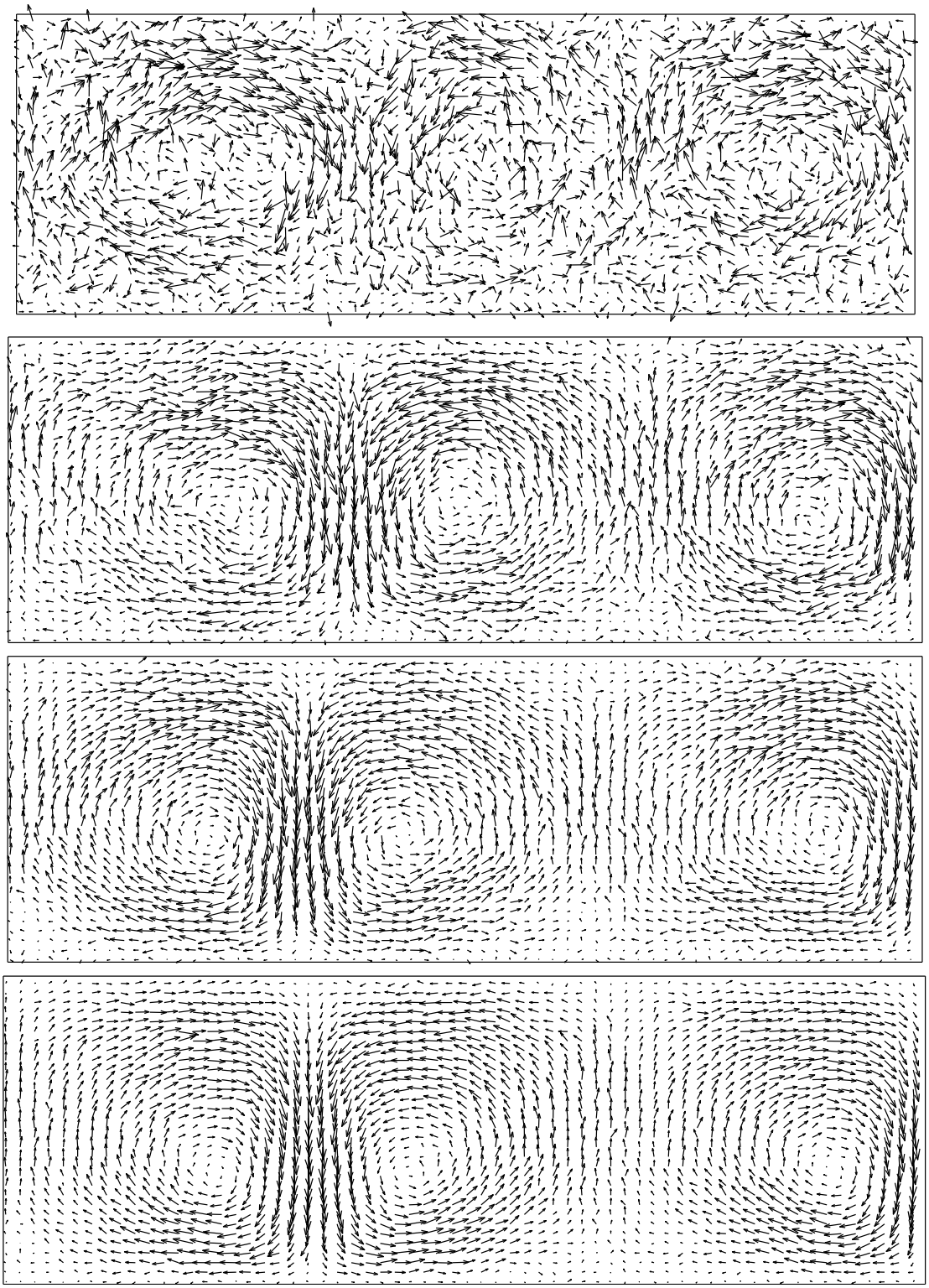

Fig. 4: Vortical structures for $Kn = 0.008$, $Fr^* = 200$ and $T_C/T_H = .4, .35, .3, .2$ sequentially

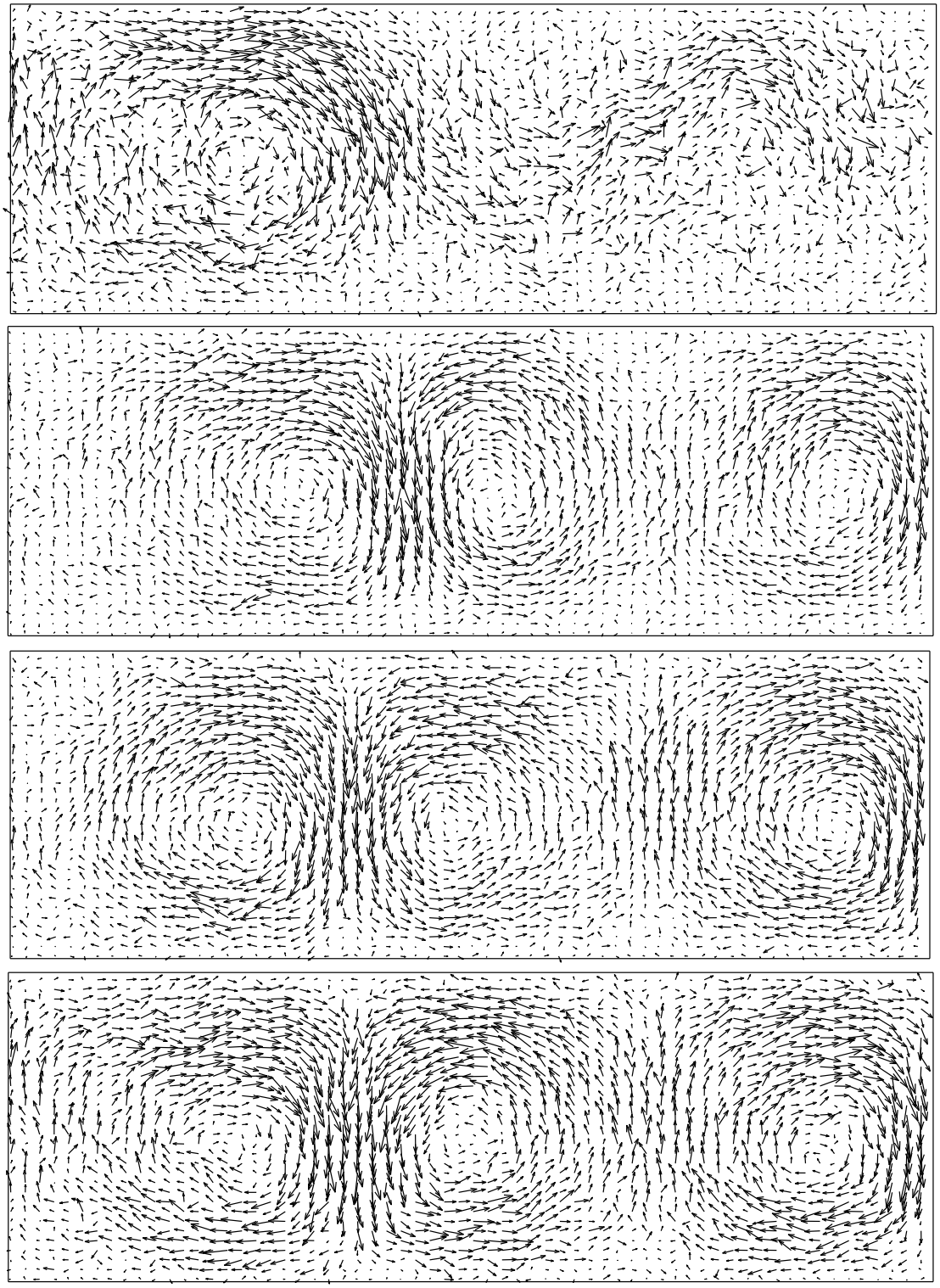

Fig. 5: Vortical structures for $Kn = 0.008$, $Fr^* = 200$ and $T_C/T_H = .35$ at different times: $t_1 = 5.0 \cdot 10^2,\ t_2 = 5.0 \cdot 10^3,\ t_3 = 1.0 \cdot 10^4,\ t_4 = 1.4 \cdot 10^4$ and mean averages over 500 time steps

The results shown in Tab. 1 and Figs. 2–5 (representatively), only give a qualitative decision whether a transition to natural convection occurs for certain values of the characteristic parameters of the problem, i.e. the temperature ratio T_C/T_H, the Knudsen number Kn and the Froude number Fr. In order to get a more quantitive insign of the first transition one may use one of the following specific quantities:

- the maximal velocity in x–direction, which should be away from zero, if vortices appear in the flow,
- the heat flux q_w at the walls, which should increase in the tranition from pure conduction to natural convection,
- the (dimensionless) Nusselt number Nu.

Concerning the last point, we have the following interpretation for the Nusselt number: if a steady state is present in the layer of depth d, than there is a constant outward heat flux from the surface at higher temperature and, if the flow across the layer is entirely due to conduction, we can write this in the form

$$q_w = \frac{k\Delta T}{d} \tag{4.1}$$

Remark 8
Actually, Eq. (4.1) only holds, if we assume that the heat conduction coefficient is independent of the temperature T. If this is not the case, the temperature difference $\Delta T = T_H - T_C$ need to be corrected by introducing an averaged temperature ratio along the layer, because we have $q_w = k\ \mathrm{d}T/\mathrm{d}x$.

An important consequence of the convective motion is an increase of the heat flux q_w across the layer. If this kind of motion is present, the resulting fluid velocity entails a supplementary heat flux and the total heat flux is higher than for the pure conductive state. This is expressed by the so–called Nusselt number Nu defined by

$$Nu = \frac{q_w d}{k\Delta T}$$

Remark 9
If we assume that the heat conduction coefficient k is independent of the temperature, we have $Nu = 1$ provided that $Ra < Ra_c$. For $Ra \geq Ra_c$, the Nusselt number increases and reflects therefore the increasing part of heat transfer due to natural convection. In the case, when the heat conduction coefficient depends on the temperature, the Nusselt number is not exactly equal to unity (see previous remark). Nevertheless, when the transition to natural convection occurs, one should observe even in this case an increase of the Nusselt number.

Fig. 6 shows, again for the particular case $Kn = 0.008$ and $Fr^* = 200$, the behaviour of the maximal velocity in x–direction as well as the heat flux q_w at the walls versus different temperature ratios T_C/T_H. The results indicate, that the transition to natural convective flow occurs around a temperature ratio $T_C/T_H = 0.4$. These results even define the critical value Ra_c of the Rayleigh number in terms of the temperature ratio at the walls.
Moreover, one may compute the corresponding behaviour of the Nusselt number Nu versus the Rayleigh number. Fig. 7 gives the results obtained from the previous curves for a Knudsen number $Kn = 0.008$, as well as for $Kn = 0.01$ and, like before, $Fr^* = 200$.

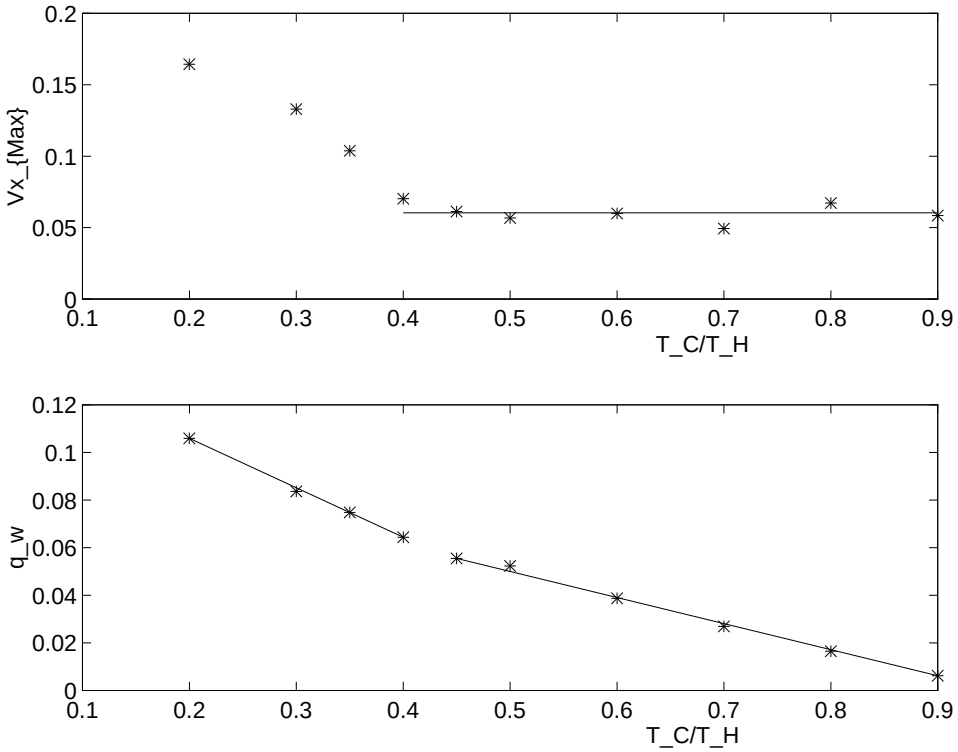

Fig. 6: Maximal x–velocity and heat flux versus the temperature ratio T_C/T_H for $Kn = 0.008$

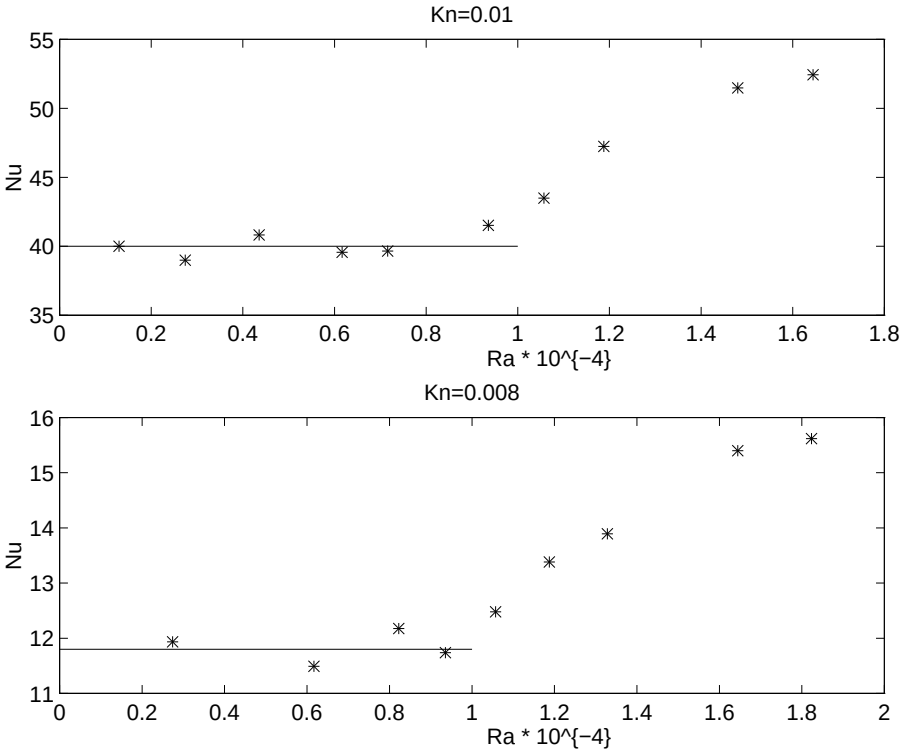

Fig. 7: Nusselt number Nu versus the Rayleigh number

At a Knudsen number $Kn = 0.008$, there is a transition for $T_C/T_H \sim 0.4$ and the corresponding critical value for the Rayleigh number is $Ra_c \sim 10.500$. On the other hand, the transition for $Kn = 0.01$ seems to occur at a smaller Rayleigh number around 8.000. This may indicate, together with the results given in Tab. 1, that the expression for the Rayleigh number given in Section 2 does not yields the same critical value Ra_c aspected from continuum theory uniformly with respect to the Knudsen number.

4.2 Two–Dimensional Simulations at Kn= 0.001

The numerical experiments presented above confirm the previous results on the existence of the Rayleigh–Bénard instability in rarefied gases given in Refs. [23] and [24]; although we are not able to validate the critical Rayleigh number $Ra_c = 1708$ from continuum flows. Besides the transition to natural convective flow, the Rayleigh–Bénard problem includes a further transition connected with the transition from regular to turbulent flows. It is out of the scope of the present paper to give a review on the existing literature for this second transition; here, we refer the reader to the textbook of Lichtenberg and Liebermann [14].
We like to mention, that this problem is connected with the existence of strange attractors on which chaotic motion takes place. This phenomena was first discovered by Lorenz [15], who studied a simplified system obtained from a truncated Fourier expansion of the Navier–Stokes equations formulated in terms of the stream function of the motion and the departure of the temperature profile from a one–dimensional one linearly decreasing with the height.
Although the Lorenz–system is a quite simplified system of the Rayleigh–Bénard problem based on only three modes in the Fourier expansion, it already contains the important phenomena of the problem: if one considers a higher number of modes, the system exhibits similar features like obtained from the Lorenz–system. Moreover, Foias and Prodi [10] showed that the solutions of the two–dimensional Navier–Stokes equations can be described asymptotically as $t \to \infty$ by a finite number of Fourier modes.
The numerical results of the previous section do not show any kind of second transition, which is in agreement with the results given by Stefanov and Cercignani in Ref. [24], where the authors even claimed, that it is impossible to simulate the transition to an unsteady turbulent motion, because the numerical simulations are completely two–dimensional. Hence, if the Rayleigh number is increased the natural convective flow stabilizes again to pure heat conduction.
In the following we give first results on a second transition to a pure unsteady behaviour with moving vortices, which indicates the existence of a strange attractor for the Rayleigh–Bénard problem in rarefied gases. The results are obtained for a Knudsen number $Kn = 0.001$, a temperature ratio $T_C/T_H = 0.1$ and a Froude number $Fr = 1$. Like in Section 4.1, the simulations are performed on a fixed spatial domain with size 300 x 100; but using a super fine grid of 1536 x 512 cells, which yields a total number of about $7.86 \cdot 10^5$ cells and a particle number of about $7.86 \cdot 10^6$. The total CPU–time to run the simulations over 32.000 discrete time steps was about 250 hrs using 64 nodes of the parallel system nCUBE 2S. This even gives a measure for the computational effort needed to run the various simulations presented in the previous section.

Remark 10
The macroscopic quantities presented in the following are calculated on 8 x 8 subcells in order to reduce the spatial fluctuations. Moreover, we used a (scaled) discrete time step $\Delta t = \Delta x/3.3$, where Δx denotes the size of a spatial cell.

Fig. 8 shows the vortical structures at different time steps during the simulation: the vortices, which at the beginning seem to be localized at the upper part of the gas layer, start to move at later times in an irregular manner through the layer.

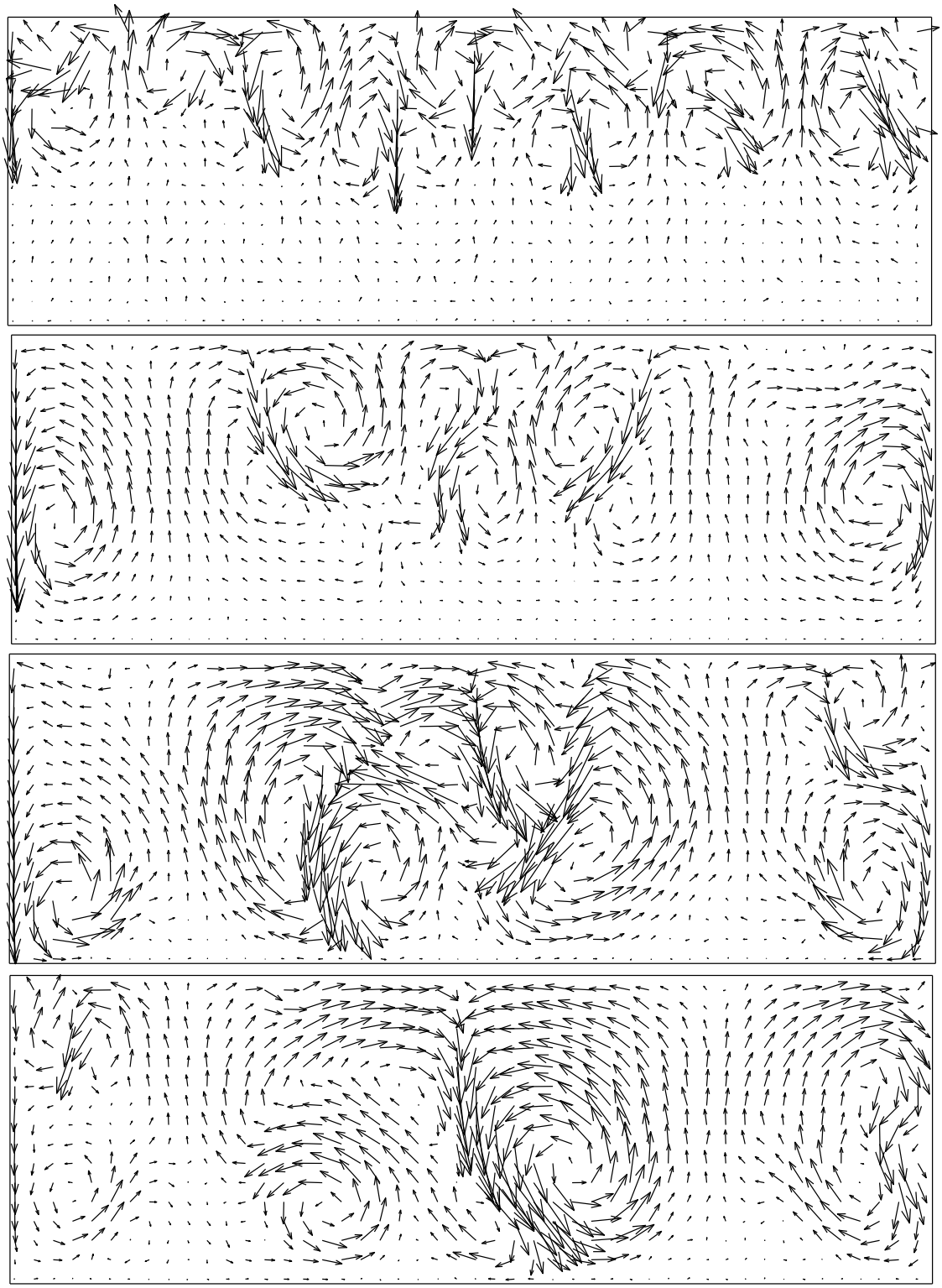

Fig. 8: Vortical structures for $Kn = 0.001$, $Fr = 1$ and $T_C/T_H = .1$ at different times: $t_1 = 1.4 \cdot 10^4,\ t_2 = 2 \cdot 10^4,\ t_3 = 2.6 \cdot 10^4,\ t_4 = 3.2 \cdot 10^4$ and mean averages over 1000 time steps

The corresponding iso–temperature lines are shown in Fig. 9: here, one observes that there exists no regular patterns like in the case of a steady convective flow with three rolls like shown in Fig. 3.

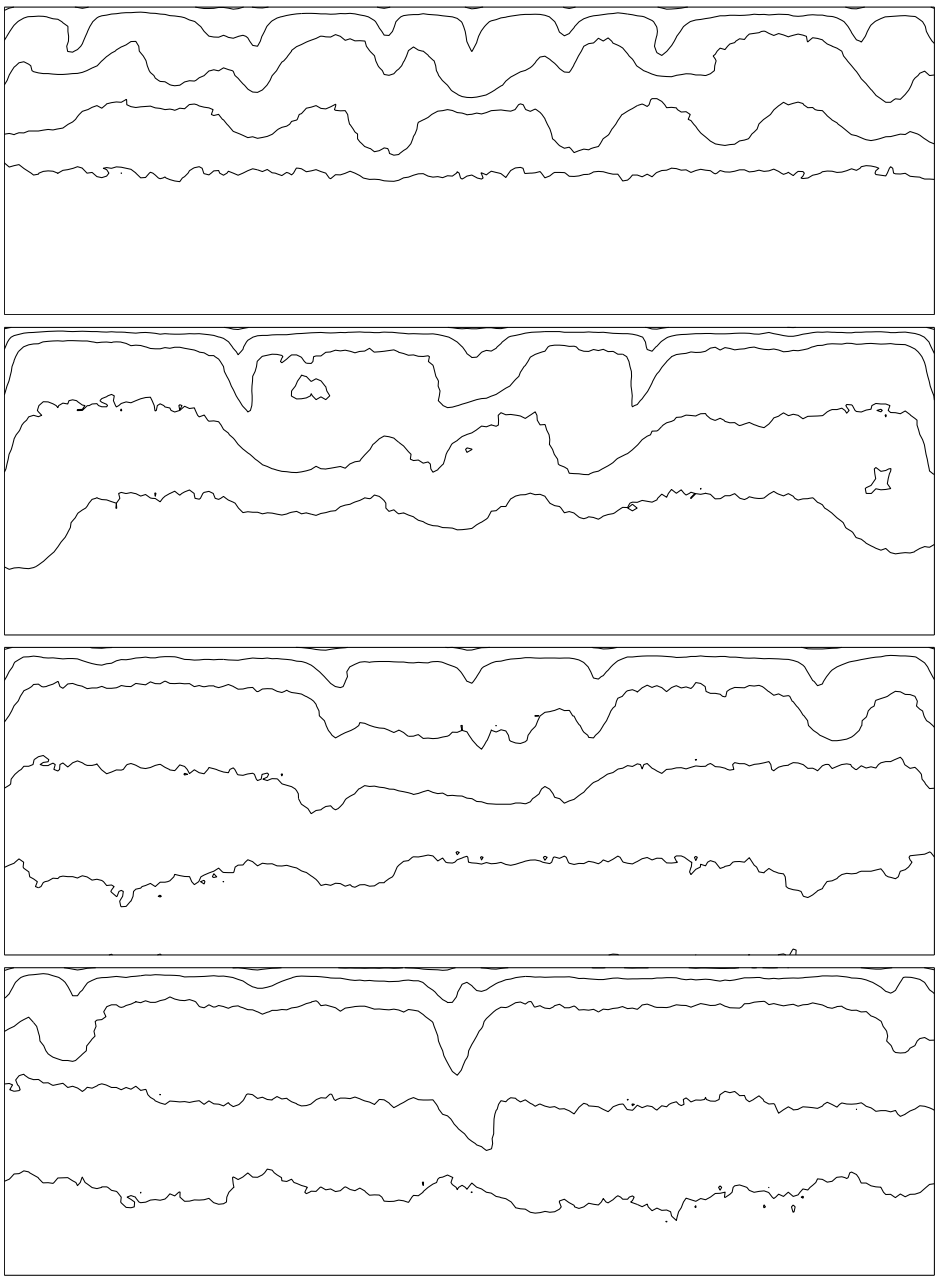

Fig. 9: Iso–Temperature Lines for $Kn = 0.001$, $Fr = 1$ and $T_C/T_H = .1$ at different times: $t_1 = 1.4 \cdot 10^4,\ t_2 = 2 \cdot 10^4,\ t_3 = 2.6 \cdot 10^4,\ t_4 = 3.2 \cdot 10^4$ and mean averages over 1000 time steps

The results shown in Fig. 8 are certainly of preliminary nature; in the sense, that one should confirm the existence of a second transition to a pure unsteady natural convective flow using further numerical experiments – although the computational effort is rather high. In particular, one should vary the Froude number to lower and higher values in order to classify the resulting flow field structure.

Moreover, it is of special interest to perform a spectral analysis for some typical flow quantities and compare the results with existing experimental data, like the one given by Gollub et al. [12]. The first results in this direction indicate, that it is necessary to perform long–time simulations, which even will increase the computational costs.

5 Conclusion

In the present investigation we studied the Rayleigh–Bénard problem in rarefied gases and confirmed the previous results on the existence of a transition to natural convective flow for various characteristic parameters. Moreover, we addressed to the question, how the Rayleigh number from continuum theory can be translated to rarefied gases and discussed how the definitions of the Rayleigh number proposed previously by various authors is related to our definition.
We were not able to validate the critical value $Ra_c = 1708$ predicted by continuum theory uniformly with respect to the characteristic parameters, i.e. the Knudsen number, the Froude number as well as the temperature ratio. Finally, the numerical simulations at a Knudsen number $Kn = 0.001$, Froude number $Fr = 1$ and temperature ratio $T_C/T_H = 0.1$ indicate the existence of a second transition to an unsteady convective flow in terms of moving vortices, which might be related with the existence of an strange attractor for the Rayleigh–Bénard problem in rarefied gases. This conjecture needs certainly to be confirmed by further numerical experiments and we will return to this point in a subsequent publication.

References

[1] G. Ahlers and R.P. Behringer, *Evolution of Turbulence from the Rayleigh–Bénard Instability*, Phys. Rev. Letters, 40 (1978), pp. 712–716.

[2] K. Aoki,*private communication.*

[3] A. Bejan, *Convection Heat Transfer*, Wiley–Interscience, New York, 1995.

[4] P. Bergé and M. Dubois, *Rayleigh–Bénard Convection*, Contemp. Phys., 25 (1984), 6, pp. 535-582.

[5] G.A. Bird *Molecular Gas Dynamics and the Direct Simulation of Gas Flows*, Clarendon Press, Oxford, 1994.

[6] C. Cercignani, *The Boltzmann Equation and its Applications*, Springer, Berlin, 1988.

[7] S. Chandrasekhar, *Hydrodynamic and Hydromagnetic Stability*, Dover, New York, 1981.

[8] S. Chapman and T.G. Cowling, *The Mathematical Theory of Non–Uniform Gases*, Cambridge University Press, 1970.

[9] N. Curle and H.J. Davies, *Modern Fluid Dynamics*, Princeton, New Jersey, Toronto.

[10] C. Foias and G. Prodi, *Sur le comportement global des solutions non-stationnaires des equations de Navier-Stokes en dimension 2*, Rend. Semin. Mat. Univ. Padova, 39 (1967), pp. 1–34.

[11] A.L. Garcia, *Hydrodynamic Fluctuations and the Direct Simulation Monte Carlo Method*, in: Microscopic Simulations of Complex Flows, ed. by M. Mareschal, Plenum Press, New York, 1990.

[12] J.P. Gollub, S.V. Benson and J. Steinmann, *A Subharmonic Route to Turbulent Convection*, in: Nonlinear Dynamics, ed. by Robert H.G. Hellemann, The New York Academy of Sciences, New York, 1980, pp. 22–27.

[13] R. Kessler, *Nonlinear Transition in Three–Dimensional Convection*, J. Fluid Mech., 174 (1987), pp. 357–379.

[14] A.J. Lichtenberg and M.A. Lieberman, *Regular and Stchastic Motion*, Springer, New York, 1983.

[15] E.N. Lorenz J. Atmos. Sci., 20 (1960), 130.

[16] M. Mareschal, *Microscopic Simulation of Instabilities*, in: Microscopic Simulations of Complex Flows, ed. by M. Marechal, Plenum Press, New York, 1990.

[17] M. Mareschal and E. Kestermont, *Order and Fluctuations in Nonequilibrium Molecular Dynamics Simulations of Two–Dimensional Fluids*, J. of Stat. Phys., 48 (1987), 5/6, pp. 1187-1201.

[18] H. Neunzert and J. Struckmeier, *Particle Methods for the Boltzmann Equation*, in: ACTA NUMERICA 1995, A. Iserles, ed., Cambridge University Press, Cambridge, 1995, pp. 417–457.

[19] H. Neunzert and J. Struckmeier, *Boltzmann Simulation by Particle Methods*, in: Boltzmann's Legacy 150 Years after his Birth, Accademia Nazionale dei Lincei, Atti dei Covegni Lincei, Roma, 131 (1997), pp. 59–78.

[20] H. Ozal and T. Hara, *Numerical Analysis for Oscillatory Natural Convection of Low Prandtl Number Fluid heated from below*, Numerical Heat Transfer, Part A, 27 (1995), pp. 307–318.

[21] A. Puhl, M. Malek Mansour and M. Mareschal, *Quantitative Comparison of Molecular Dynamics with Hydrodynamics in Rayleigh–Bénard Convection*, Physical Review A, 40 (1990), 4, pp. 1999–2011.

[22] Lord Rayleigh, *On convective currents in a horizontal layer of fluid when the higher temperature is on the under side*, Philos. Mag., 32 (1916), pp. 529–546.

[23] Y. Sone, K. Aoki, H. Sugimoto and H. Motohashi, *The Bénard Problem of Rarefied Gas Dynamics*, in: Rarefied Gas Dynamics, Proc. of the 19th International Symposium, ed. by J. Harvey and G. Lord, Oxford University Press, 1995, pp. 135–141.

[24] S. Stefanov and C. Cercignani, *Monte Carlo Simulation of Bénard's Instability in a Rarefied Gas*, Eur. J. Mech., B/Fluids, 11 (1992), pp. 543–554.

[25] J. Struckmeier, *A Steady–State Particle Method for the Boltzmann Equation*, Preprint, University of Kaiserslautern, 1998, submitted for publication.

[26] J. Struckmeier and F.J. Pfreundt *On the Efficiency of Simulation Methods for the Boltzmann Equation on Parallel Computers*, Parallel Computing, 19 (1993), pp. 103–119.

[27] J. Toomre, D.O. Gough and E.A. Spiegel, *Time–dependent solutions of multimode convection equations*, J. Fluid Mech., 125 (1982), 99-122

[28] T.–S. Wung and F.–G. Tseng, *A Color–Coded Particle Tracking Velocimeter with Application to Natural Convection*, Experiments in Fluids, 13 (1992), pp. 217–223.